ENVIRONMENTAL RESEARCH
LETTERS

CrossMark

LETTER

Assessing local CO$_2$ contamination revealed by two near-by high altitude records at Jungfraujoch, Switzerland

Stéphane Affolter[1,2,8] , Michael Schibig[2], Tesfaye Berhanu[2,3], Nicolas Bukowiecki[4,8] , Martin Steinbacher[5], Peter Nyfeler[2], Maxime Hervo[6], Jürg Lauper[7] and Markus Leuenberger[1,2]

[1] International Foundation High Altitude Research Stations Jungfraujoch and Gornergrat (HFSJG), Bern, Switzerland
[2] Climate and Environmental Physics, Physics Institute and Oeschger Centre for Climate Change Research, University of Bern, Bern, Switzerland
[3] Picarro Inc., 3105 Henry Patrick Dr, Santa Clara, CA, United States of America
[4] Laboratory of Atmospheric Chemistry, Paul Scherrer Institute, CH-5232 Villigen, PSI, Switzerland
[5] Empa, Swiss Federal Laboratories for Materials Science and Technology, Dübendorf, Switzerland
[6] Federal Office of Meteorology and Climatology MeteoSwiss, Chemin de l'Aérologie, 1530 Payerne, Switzerland
[7] Jungfraubahnen, Harderstrasse 14, Interlaken, Switzerland
[8] Present address: Department of Environmental Sciences, University of Basel, Basel, Switzerland

E-mail: stephane.affolter@unibas.ch

Keywords: CO$_2$, high altitude, anthropogenic impact, touristic infrastructure

Supplementary material for this article is available online

Abstract

Remote research stations are guarantor of high-quality atmospheric measurements as they are essentially exposed to pristine air masses. However, in a context of increasing touristic pressure for certain sites, attention should be paid to the local anthropogenic emission related to the infrastructure itself. Among emissions, carbon dioxide (CO$_2$) is the most important anthropogenic greenhouse gas and a major contributor to the current global warming. Here, we compared two years of CO$_2$ dry air mole fraction records from Jungfraujoch (Swiss Alps) measured at the Sphinx Laboratory (3580 m a.s.l.; JFJ) and the East Ridge facility (3705 m a.s.l.; JER; horizontal distance of ~1 km), respectively. Both stations show an overall increase of the annual mean CO$_2$ mole fraction in line with current global trends. On a daily basis, values during the night (00h00–06h00) show robust coherence with variability ranging within the measurement uncertainties matching the WMO compatibility goal of 0.1 ppm, which we considered to be background air CO$_2$ mole fraction for Central and Western Europe. However, JFJ record shows superimposed short-term variability with diurnal CO$_2$ spikes centered around noon. Whereas the variability occurring during time intervals ranging from days to weeks seem to be driven by inputs of air masses from the planetary boundary layer, we suppose that the super-imposed diurnal CO$_2$ spikes occurring essentially in summer are explained by local emission sources related to the infrastructure (visitors, tourism, etc). Nevertheless, we cannot point to a single triggering cause for those spikes as it probably results from a combination of factors. In order to minimize these local emissions, smooth collaboration between all the involved stakeholders is required.

1. Introduction

Being built in 1937, there is a long history of research at the Sphinx Laboratory of the High Altitude Research Station Jungfraujoch (JFJ hereafter) located in the Swiss Alps (Balsiger and Flückiger 2016). Currently, it is hosting numerous research projects from international institutes (HFSJG 2019) and constitutes a lead location for atmospheric measurements in Europe. It allows to measure the chemical composition of atmospheric air and to document thereby driven climate change (Vollmer *et al* 2015, 2016, Buchmann *et al* 2016, Bukowiecki *et al* 2016, Schibig *et al* 2016, Mahieu *et al* 2017) or to understand cloud formation (Kirkby *et al* 2016, Tröstl *et al* 2016). A key feature of the site is the remote setting and its exposure to pristine air masses with only sporadic air mass transport originating from the surrounding lowlands
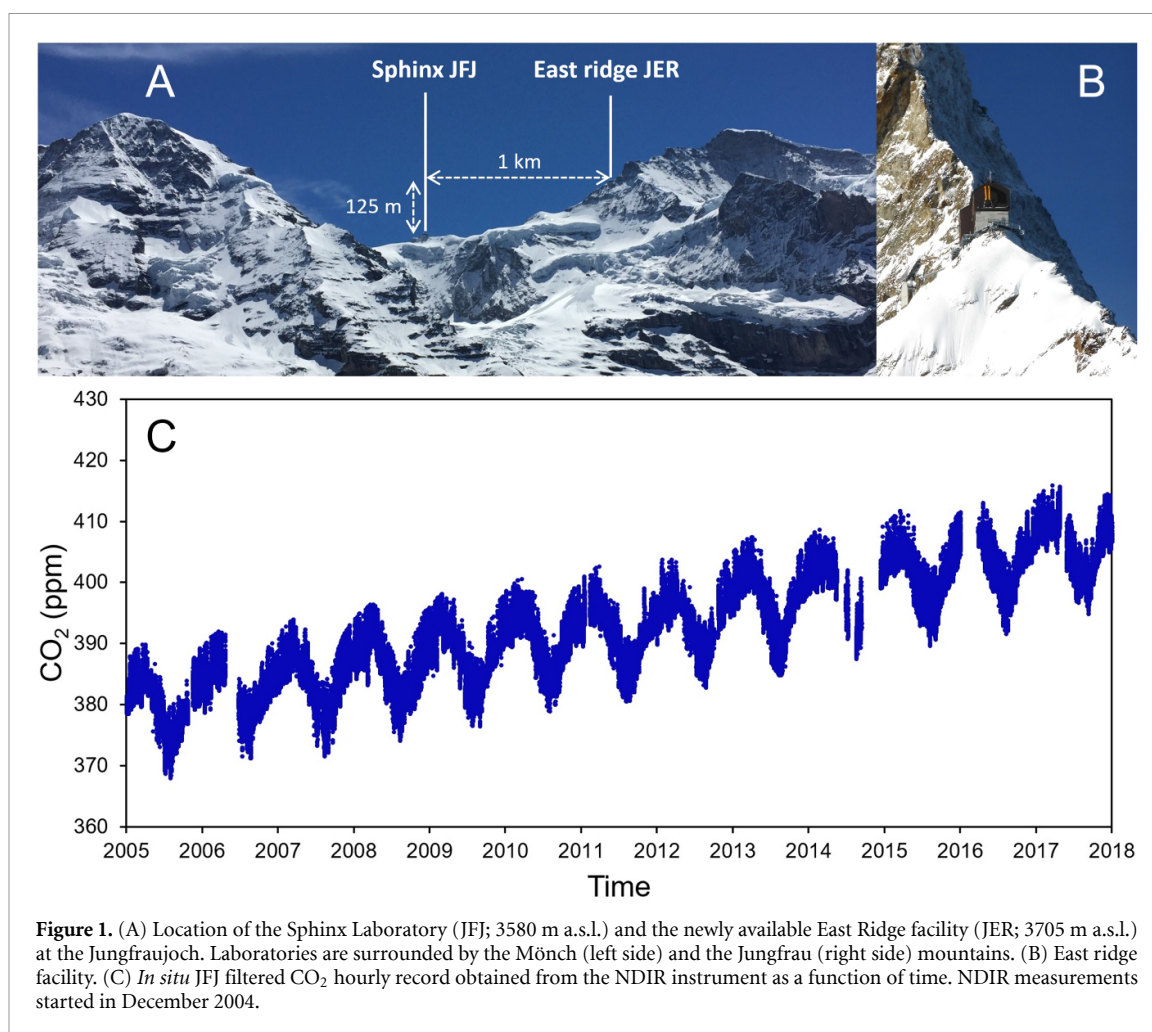
Figure 1. (A) Location of the Sphinx Laboratory (JFJ; 3580 m a.s.l.) and the newly available East Ridge facility (JER; 3705 m a.s.l.) at the Jungfraujoch. Laboratories are surrounded by the Mönch (left side) and the Jungfrau (right side) mountains. (B) East ridge facility. (C) *In situ* JFJ filtered CO_2 hourly record obtained from the NDIR instrument as a function of time. NDIR measurements started in December 2004.

set in the atmospheric boundary layer inducing pollution events (Baltensperger *et al* 1997, Henne *et al* 2010, Bukowiecki *et al* 2016). In December 2014, an additional facility was established at the Jungfrau East Ridge (JER) building that is set on the East Ridge of the Jungfrau Mountain 125 m higher and 1 km westward of JFJ (figure 1). This new location is currently not publicly accessible and represent a valuable location to extend the measurement possibilities of the station (Buchmann *et al* 2015). Moreover, JER allows for a quality survey of JFJ due to the lack of human pollution and all activities inherent to the touristic exploitation of the Jungfraujoch area. The number of visitors doubled in the last 10 years and reached 1 million for the first time in 2015. Since, 1 million were also achieved in 2017, 2018 and 2019.

CO_2 (given hereafter in ppm, where ppm corresponds to μmol mol^{-1} in dry air) is a major greenhouse gas that contributes to a large extent to the radiative forcing of the Earth's atmosphere (IPCC 2013). Since the industrial revolution, the atmospheric CO_2 mole fraction has been increasing continuously from a relatively stable pre-industrial CO_2 mole fraction level of $\sim$280 ppm to reach a global abundance of

407.8 ppm in 2018 (WMO 2019). The Intergovernmental Panel on Climate Change (IPCC 2013) stated that the atmospheric CO_2 increase is clearly due to anthropogenic activities and due to its greenhouse gas properties, the additional CO_2 contributes to the global warming by about $\sim$1.0 °C of the mean atmospheric temperature increase. Time series of CO_2 measurements are recorded worldwide and most data (including JFJ records) are available online at the WMO's World Data Centre for Greenhouse Gases (https://gaw.kishou.go.jp). Usually, high altitude sites act as reference sites as signals from specific sources (like anthropogenic emissions from industry, traffic and households, etc) are not directly but smoothly recorded by integration over the time due to atmospheric mixing during advection. At JFJ, CO_2 is continuously measured since 2004 with initial values of $\sim$375 ppm and an annual increase of $\sim$2 ppm (van der Laan-luijkx *et al* 2013, Schibig *et al* 2016). The JFJ record shows also seasonal variations of around 10 ppm with maximal CO_2 values in March–April and minimal values in August–September. Generally long-term trend CO_2 variations are due to anthropogenic emissions whereas seasonal variability is induced by variations in diurnal solar

radiation and related CO_2 uptake and release by the biosphere (IPCC 2013).

While technical specifications of available instrumentation along with adequate calibration strategies allow to meet the WMO compatibility goal of 0.1 ppm (WMO 2020), the influence of local contamination in such remote areas needs to be quantified (e.g. Loov *et al* 2008, Ruckstuhl *et al* 2012). In addition, several studies focused on the advection of lower atmospheric layers to the elevation of the sampling sites (e.g. Griffiths *et al* 2014, Tsamalis *et al* 2014, Ferrarese *et al* 2015, Fu *et al* 2016). Moreover, conditions and the degree of impact depend on the specific characteristics of the sampling site and the parameter of interest. For example, measurements performed at Mount Zugspitze, Germany, observed that an increased number of visitors on the weekends do not correspond to higher levels of CO_2 suggesting that CO_2 mixing ratios are not significantly influenced by neighboring touristic activities, at least with only 100–200 visitors per day (Yuan *et al* 2019). There are numerous high alpine stations running high precision measurements (e.g. Monte Rosa, Schneefernerhaus, Sonnblick, etc). Some of which host touristic infrastructures in parallel (e.g. JFJ, Schneefernerhaus), which constitutes a source of contamination as visitors are breathing, smoking and consuming onsite. Moreover, transport to the site requires helicopter flights, trains, cabins as well as infrastructure that all need regular maintenance or construction work. Together with the companion paper about aerosol measurements (Bukowiecki *et al* 2021), the greenhouse gas observations presented here allow for an investigation of anthropogenic contamination, but also an insight into the tourism increase issue.

2. Settings and method

The Jungfraujoch (46.5475° N/7.9852° E) is a saddle in the Swiss Alps separating the Jungfrau (4158 m a.s.l.) and the Mönch (4107 m a.s.l.) mountains. JFJ Sphinx laboratory (3580 m a.s.l.) is set at the Jungfraujoch, whereas JER (3705 m a.s.l.) is located SW on the ridge leading to the Jungfrau summit (figure 1). Due to their proximity, the two locations are considered to experience similar regional weather conditions. The Jungfraujoch is often situated in the free troposphere which allows measurements of atmospheric background CO_2 mole fractions. Punctual convective transport of polluted valley air masses occurs mainly during the afternoon and predominantly during the warm season (Sturm *et al* 2005, Bukowiecki *et al* 2016, Poltera *et al* 2017). Local wind direction is driven by the local topography resulting in two prevailing wind directions (NW and SE) and interactions with the mountainous topography may lead to variations between both locations as JFJ is situated on the saddle and the JER building is

higher up on the mountain ridge. Therefore, uplifted air masses should generally first cross JFJ before reaching JER.

The air inlet feeding the CO_2 analyzer at JFJ is placed on the roof of the Sphinx building ∼8 m above a touristic terrace where people can experience an outstanding view and where smoking was not discouraged. Since the end of 2016 panels inform the visitors about sensitive measurements just above their heads and ask them to refrain from smoking. It is relevant when up to 5000 visitors per day reach the site, 5–6 times more in summer than in winter. The JFJ laboratory is set ∼150 m away from the main recreational area that consists of restaurants, shops and a train station. The Sphinx building can be reached with elevators (108 m elevation). The elevator shaft is likely facilitating the transport of air from the underground tunnel complex upwards, which may have an influence on the measurements. It is noteworthy that there are only moderate CO_2 emissions from the infrastructure itself since most units run on electricity, with exceptions only during construction phases. At JER, the CO_2 analyzer was placed in an empty room of the former telecommunication building that is now available for scientific purposes. During the measurement campaign, this facility was visited only occasionally and exclusively by scientists and maintenance staff. JER is reachable by a tunnel starting from the Jungfraujoch main train station, where the air is regularly vented upwards and outside.

We scaled the number of people visiting the Jungfraujoch available as daily totals using the mean annual visitor percentage per hour (arriving onsite) in order to approximate the diurnal cycle of visitors, which do not absolutely mimic reality. The planetary boundary layer (PBL hereafter) data was measured by MeteoSwiss using a ceilometer based at the Kleine Scheidegg (2061 m. a.s.l.) below the Jungfraujoch (Poltera *et al* 2017). To be noted, PBL influence is likely to occur even if its height is below JFJ elevation due to shallow upslope injections not resolved by the ceilometer. Thus, we use in addition black carbon (BC) as another indicator for advection of boundary layer of air masses, measured as equivalent black carbon (eBC) mass concentrations, see detailed description in the companion paper (Bukowiecki *et al* 2021).

To perform CO_2 measurements at JER, we use a Picarro G2311-f analyzer based on the Cavity Ring-Down Spectroscopy (CRDS) technology installed in December 2014. At JFJ we use a nondispersive infrared (NDIR) gas analyzer (Sick Maihak model S710; see supplementary information (available online at stacks.iop.org/ERL/16/044037/mmedia)). Finally, we also used methane (CH_4) and carbon monoxide (CO) records measured with Picarro G2401 by the EMPA at both sites between December 2014 and May 2016.
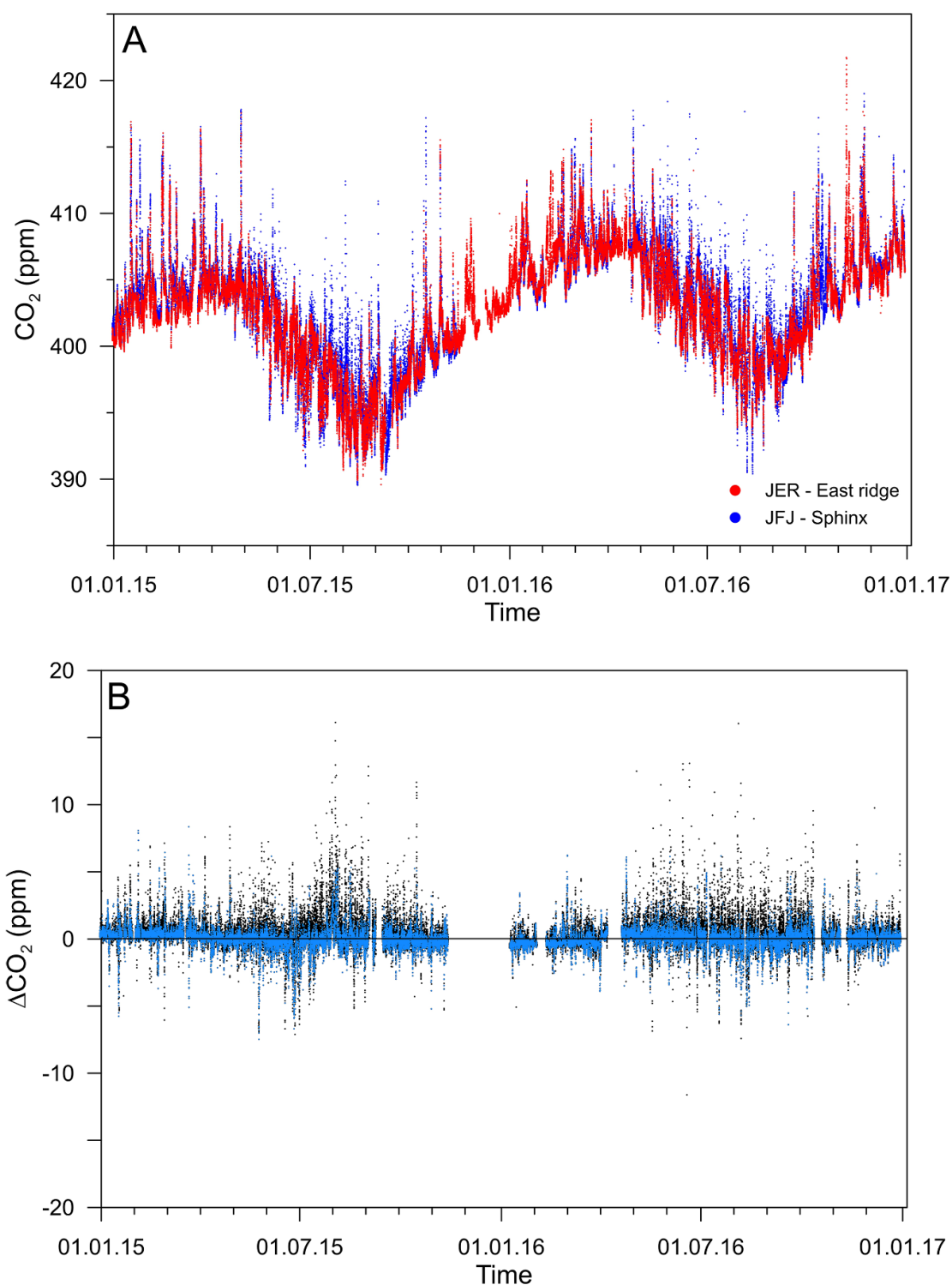
Figure 2. (A) CO_2 measurements recorded over 2 years at JER with a CRDS instrument (red) and JFJ using a NDIR instrument (blue). The values correspond to 6 min averages for both measurement systems. (B) Difference between the two CO_2 records (JFJ minus JER) based on 6 min averages measurement values. Nighttime values are highlighted in blue.

3. Results and discussion

The JFJ CO_2 *in situ* record (figures 1 and 2) constitutes the extension of the measurement started in December 2004 (Schibig *et al* 2016). The record is robust and shows similar results in trend and amplitude compared to JER. Over the 2 years values ranged between 390 and 419 ppm at JFJ and between 390 and 422 ppm at JER. The JFJ CO_2 record (figure 1) shows a mole fraction increase of 2.22 ± 0.04 ppm yr^{-1} during the interval 2005–2018 as calculated with a Monte Carlo algorithm. This value is significantly higher than the previous published slope of 1.97 ppm yr^{-1} obtained for the interval 2005–2013 (Schibig *et al*

2016) and result from strong annual mean CO_2 growth rate over the last decade (Friedlingstein *et al* 2019, WMO 2019). The seasonality obtained by the difference between the highest (March–April) and the lowest (August) detrended monthly average is 10.72 ± 1.00 ppm, similar as previously determined. The JER record is too short to determine robust trend and annual seasonality.

3.1. Comparison JER–JFJ and robust night values
The comparison between NDIR and CRDS records is robust ($R^2 = 0.94$ in overall and $R^2 = 0.96$ for night values, slope of ∼1; figure 3(A)) and the agreement is good over the 2 years (figure 2) either in minima or maxima events despite the relative distance (∼1 km) between the two sites and documents a similar annual CO_2 increase. Nevertheless, a mean CO_2 excess (values at JFJ minus values at JER) with normal distribution is observed (figure 3(B)), which is higher than what can be expected due to the different NDIR and CRDS measurement techniques (Schibig *et al* 2015). When splitting data of the days into two categories named daytime (06h00–18h00) and nighttime (18h00–06h00), the values emphasize the differences between the two sites with $+0.49$ ppm and only $+0.01$ ppm, respectively. The mean CO_2 excess (figure 3(B)) is essentially due to the addition of positive CO_2 excursions during daytime observed at JFJ. These excursions occur almost daily during the warm season, essentially May to September between 8h00 and 17h00 when visitors are onsite, whereas from October to April, they are less likely to occur and also less pronounced (figure 4 and supplementary figure 1). The short-term diurnal maximal offset is generally up to ∼5–10 ppm for a couple of hours around noon. During the night, focusing on the interval 00h00–06h00, values are in excellent agreement independent of the day of the week and within the internal variability of the two instruments (± 0.1 ppm) (figures 5 and 6), which supports our expectations that the two sites are experiencing the same meteorological conditions during the night and measure the same air. Since JFJ measurements are considered to be robust CO_2 atmospheric background values during the night, we can assume the same for JER. When visitors are onsite, the daily differences are ranging between 0.3 and 0.7 ppm (figure 5).

At JER, the CO_2 record shows less variability during the raising concentration phase in autumn and winter 2015 and 2016 (figure 2(A)). From roughly 15th September to 16th February, the reduced variability may be a result of the fact that the Jungfraujoch and East Ridge area is predominantly in the free troposphere, which is supported by PBL data (Poltera *et al* 2017). JFJ shows a slightly more variable pattern indicated by the spikes in the difference between the two records (figure 2(A)).

In addition, low values seem to occur mainly in spring and summer at around noon until early afternoon (∼12h00–16h00; figure 2). Thus, during these events JFJ (and to a smaller extent JER as it is higher) is influenced by air masses coming from the boundary layer. Boundary layer air masses in spring and summer are expected to be depleted in CO_2 due to photosynthetic uptake and reduced anthropogenic emissions (e.g. due to no domestic heating). The (negative) differences are likely a consequence of a sampling of different air masses at JFJ and JER. Such events are not unlikely due to the local wind patterns caused by the complex topography.

A few other observations seem to be of recurring nature, yet sometimes equivocal. Synoptic events affect both locations at the same time as seen for instance in supplementary figure 1 (16th and 17th January 2015) and correspond to regional events such as input of polluted air masses from the lower Grindelwald valley or large-scale European patterns such as events driven by wind coming from the south, i.e. South Föhn. These air masses show another CO_2 signature as the well mixed Atlantic CO_2 background values. Generally, Föhn events result in variable CO_2 mole fraction compared to more stable values when air masses are coming from the northern sector. Another observation is that when the PBL is reaching Jungfraujoch (mostly in summer), we may observe a drop in the CO_2 mole fraction in summer and vice versa (see section 4.2; Uglietti *et al* 2011).

The seasonal differences for CO_2 spikes in the time series for summer and winter in 2015 and 2016 are clearly visible (figure 4 and supplementary figure 1). The two summer examples show the same pattern with diurnal spikes at JFJ in contrast to JER, with maximal spike values of ∼10 ppm. These spikes start at ∼08h00 at the time or slightly before the arrival of the trains with a maximum value around noon. Winter values clearly show a distinct behavior with reduced spike number occurrence—if any—and lower amplitudes. Both years show identical nighttime values and behavior during the days in January 2015 and 2016.
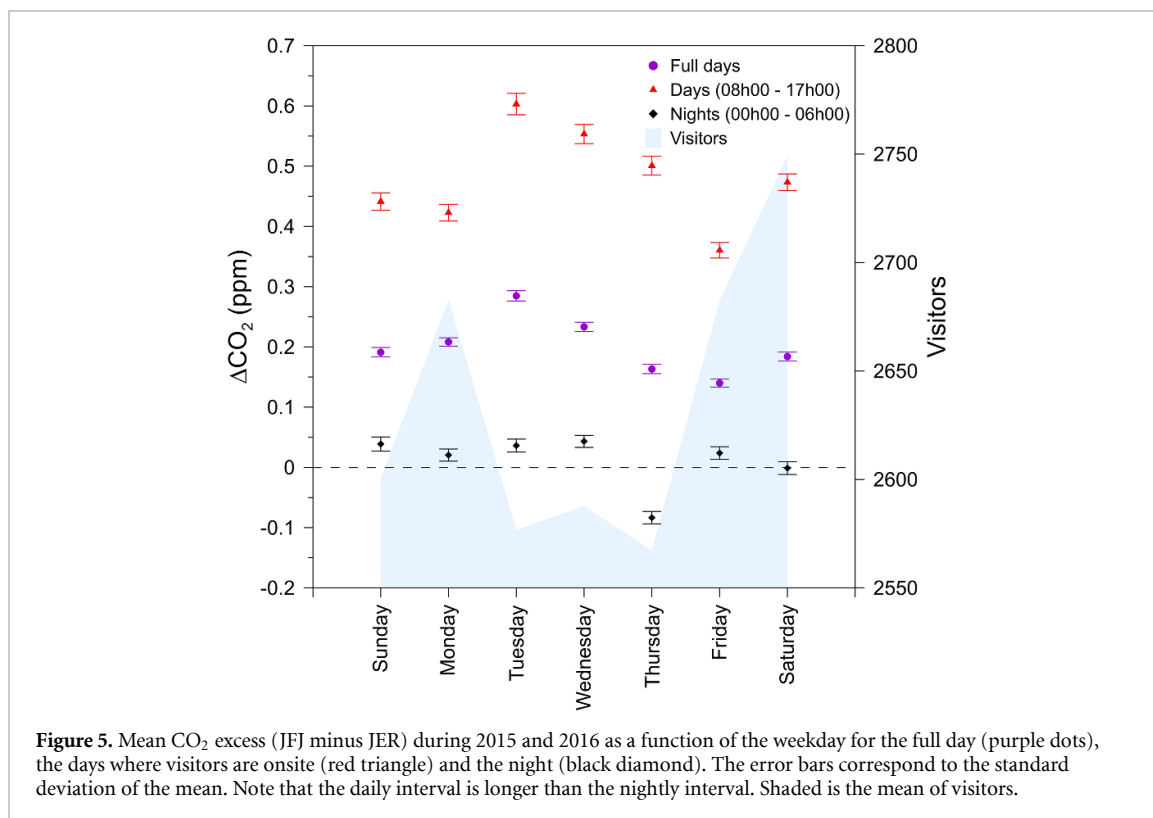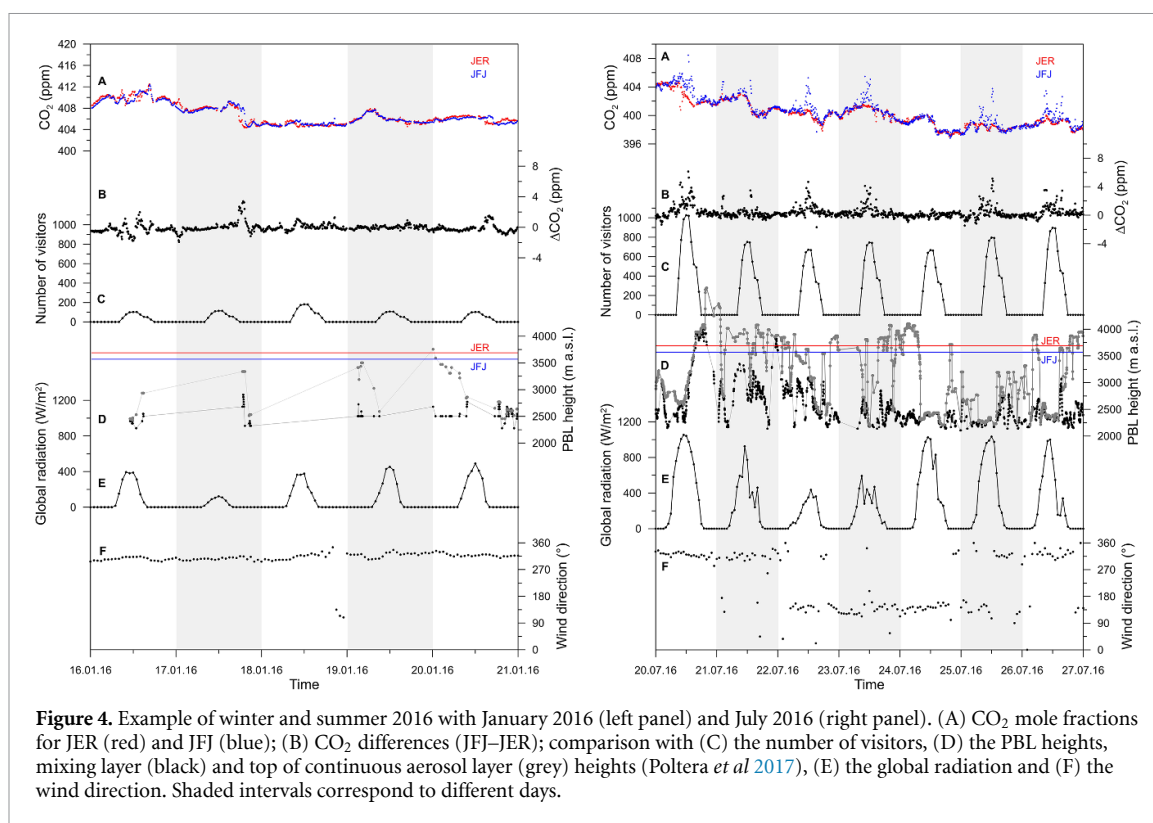
3.2. Comparison with PBL, eBC, CO and CH_4
We observed no similarities between convective strength from the valley (PBL inputs) as resolved by the ceilometer and CO_2 spikes (figure 4 and supplementary figure 1). As shallow upslope injections cannot be detected by the ceilometer, we further characterize the influences of air masses uplifts based on eBC inputs at both sites (Bukowiecki *et al* 2021). eBC is mostly produced in the PBL through incomplete combustion of fossil fuel or biomass burning (Petzold *et al* 2013). Locally, construction works or preparation of the touristic infrastructure on the glacier with snowcat operations
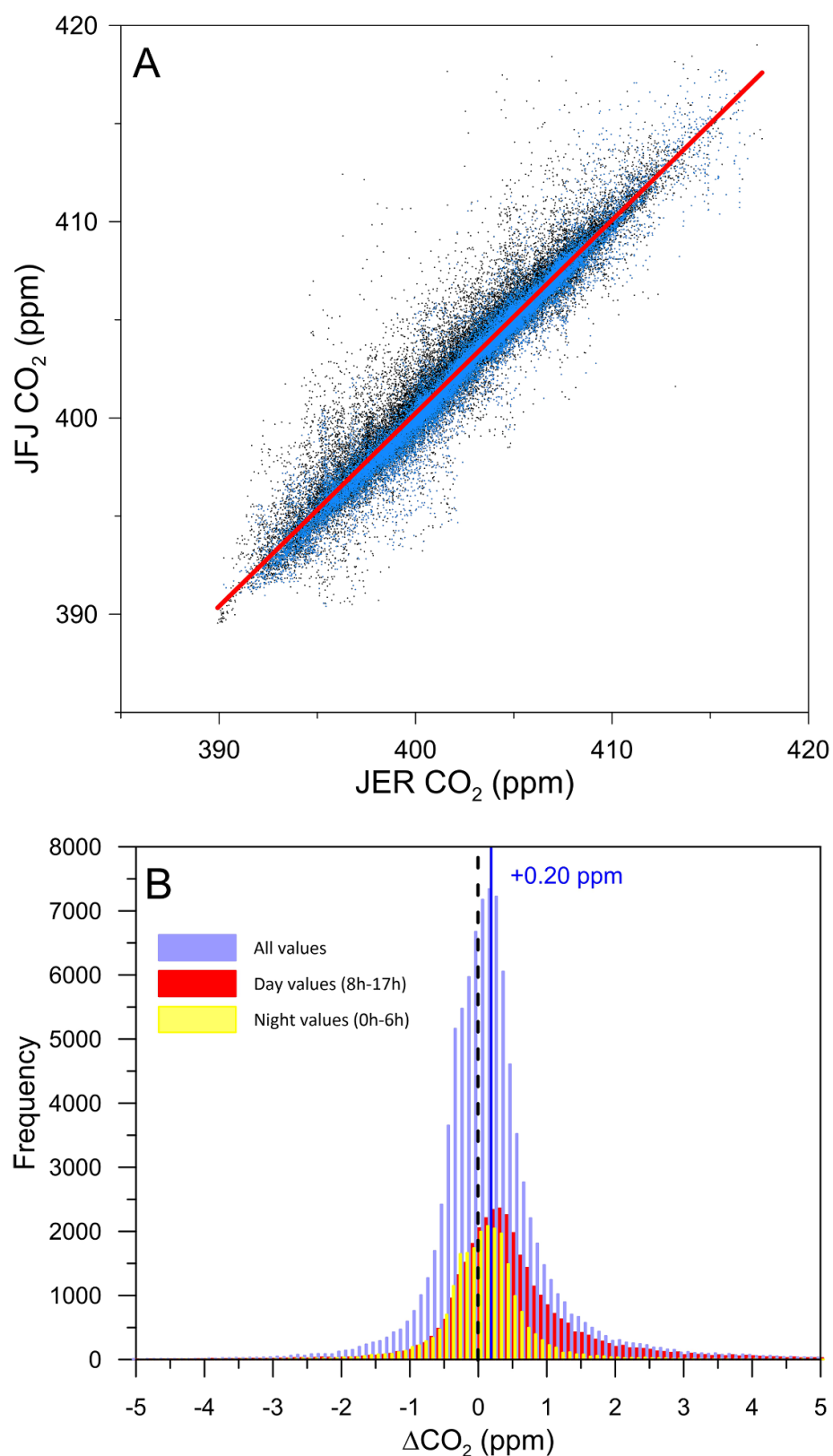
Figure 3. (A) JFJ versus JER CO_2 mixing ratios based on 6 min average values. Nighttime values are highlighted in blue. (B) Frequencies of CO_2 excess values. The blue line indicates the mean excess over the 2 years of measurements. Daily values when visitors are onsite (red) and nightly values between 00h00 and 06h00 (yellow) are also shown.

also contribute to local eBC emission (Bukowiecki *et al* 2016). Minor contamination from tobacco smoke was also shown through the correlation between corresponding environmental markers and

the number of visitors in August (Frohlich *et al* 2015). Theoretically, only low eBC concentration should be recorded at JFJ due to the remote location and the fact that JFJ is essentially in the free troposphere.

Figure 4. Example of winter and summer 2016 with January 2016 (left panel) and July 2016 (right panel). (A) CO_2 mole fractions for JER (red) and JFJ (blue); (B) CO_2 differences (JFJ–JER); comparison with (C) the number of visitors, (D) the PBL heights, mixing layer (black) and top of continuous aerosol layer (grey) heights (Poltera *et al* 2017), (E) the global radiation and (F) the wind direction. Shaded intervals correspond to different days.

Figure 5. Mean CO_2 excess (JFJ minus JER) during 2015 and 2016 as a function of the weekday for the full day (purple dots), the days where visitors are onsite (red triangle) and the night (black diamond). The error bars correspond to the standard deviation of the mean. Note that the daily interval is longer than the nightly interval. Shaded is the mean of visitors.

eBC increase indicates events when JFJ is contaminated by air masses coming from the PBL or by local emissions. To distinguish these two sources, we compare the two site records since local emissions are pre-dominantly seen only at the Sphinx observatory. The comparison between eBC and CO_2 shows that both records evolve often similarly and thus explain a significant part of the short-term variability (days to weeks). A striking observation is shown in figure 7 which highlights the different influence of the PBL input in winter and summer. In February 2015 and 2016, positive excursions in the CO_2 mixing ratio
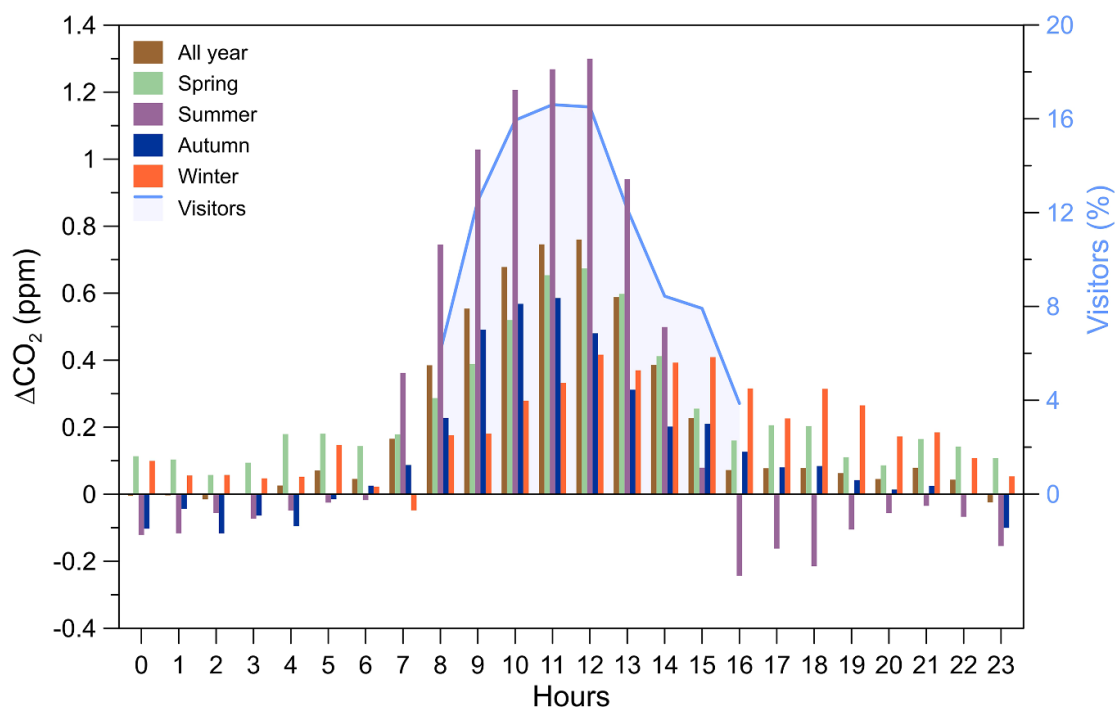
Figure 6. Excess CO_2 for years 2015 and 2016 versus time of day sub-divided into seasons. The hourly mean percentage of visitors arriving at JFJ for the year 2015 is also shown (secondary axis, light blue). Differences during the night are stable within the measurement uncertainty of ± 0.1 ppm.
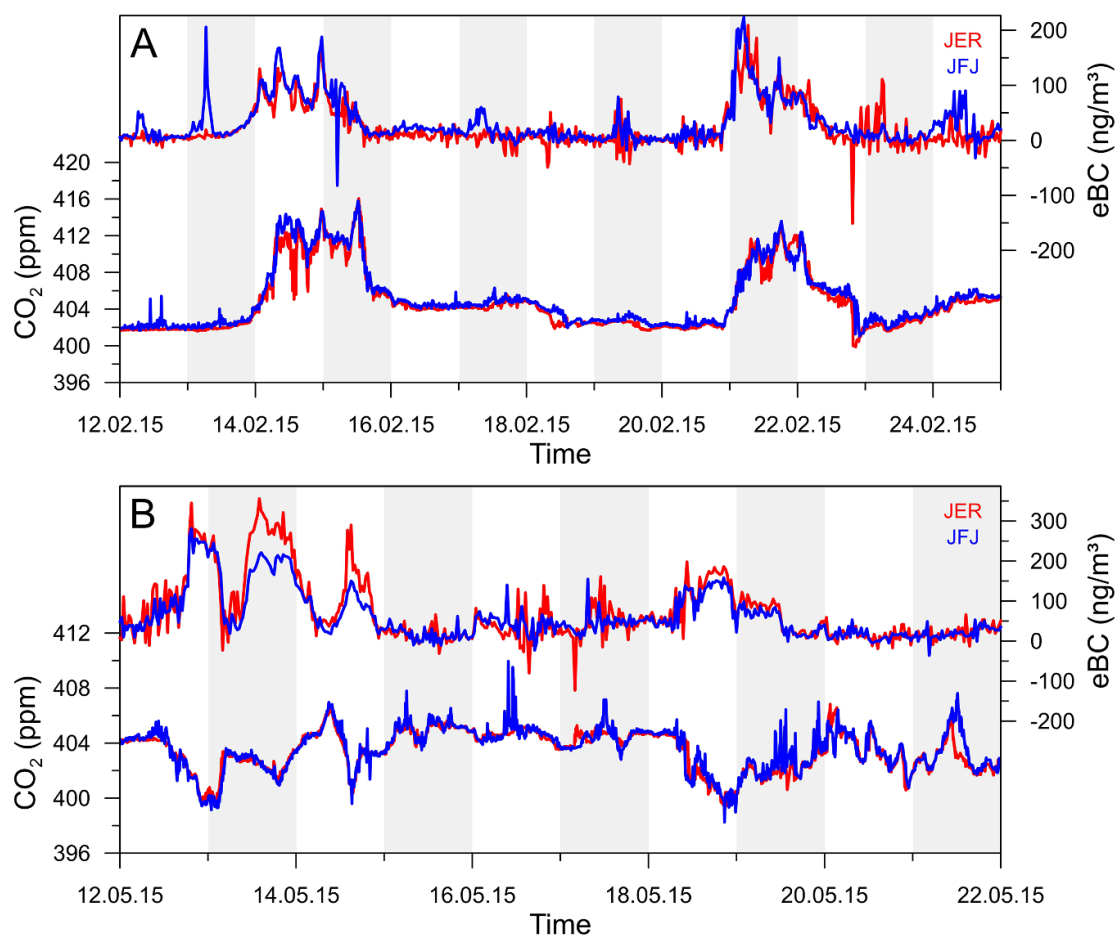
Figure 7. Comparison between CO_2 and black carbon (eBC) records between JER (red) and JFJ (blue) for (A) winter and (B) spring. Shaded intervals correspond to different days.
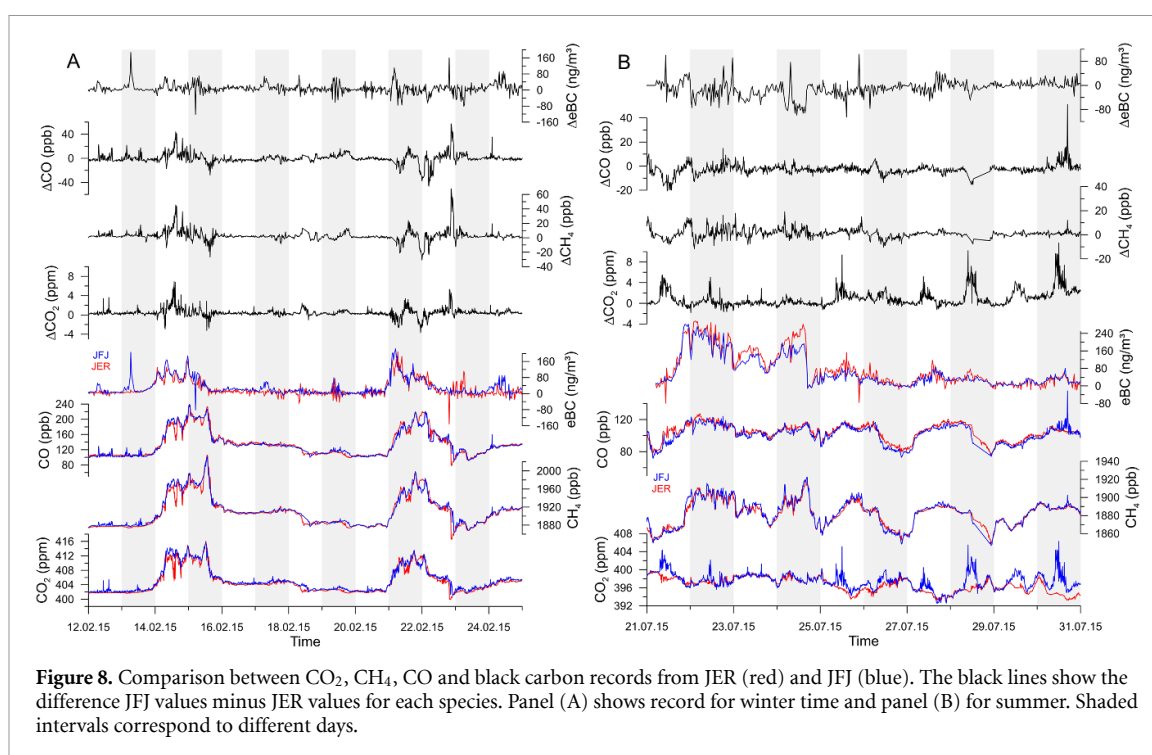
Figure 8. Comparison between CO_2, CH_4, CO and black carbon records from JER (red) and JFJ (blue). The black lines show the difference JFJ values minus JER values for each species. Panel (A) shows record for winter time and panel (B) for summer. Shaded intervals correspond to different days.

at both sites occur similarly to the increase in eBC content which means that uplifting of polluted air masses from the PBL (due to heating, traffic, etc) enhance the increase of the CO_2 mixing ratio due to vegetation respiration in winter. On the contrary, in spring and summer (for instance in May and June 2015) when large inputs of eBC occurred, we observe a decrease of the CO_2 mixing ratio due to the uplift of air masses from the valley depleted in CO_2 caused by ongoing photosynthesis (Uglietti *et al* 2011). While this example shows variation on a day or a couple of days, multi-weeks trends as for instance observed in July 2015, show also such a dependence with slight increase of the eBC content occurring at the same time as a continuous decreasing trend in the CO_2. Nevertheless, superimposed are still daily variations on most of the summer days that are not correlated to eBC variations as for instance shown for July 2015 (figure 8(B)). Local emission CO_2 and eBC sources do not have to be related, e.g. breath air in contrast to emissions from construction, snowcat or smoking.

Occasionally, a higher eBC increase can be observed at JFJ compared to JER. This could be caused by either local contamination at JFJ or by local wind processes, leading to the situation that JFJ is situated within the PBL while JER remains above.

Comparison with CO and CH_4 records (figure 8) leads to interesting observations. CO is only related to anthropogenic emissions essentially produced by incomplete burning of fossil fuels or biomass (Dils *et al* 2011). In winter the short-term variability in both absolute values and in the difference between

JFJ and JER are very similar, which support our suggestion that most CO_2 short-term variability can be explained by variations in wind regimes, essentially by PBL height variability. For example, in January and February 2015 all four atmospheric compounds evolve similarly on a visual basis (figure 8). And thus, single CO_2 spikes are less likely to be observed. In summer, the situation is slightly different as BC, CO and CH_4 are visually correlated and CO_2 shows negative correlation for the aforementioned reasons. However, in summer superimposed to this variability, single CO_2 spikes were observed with maximal values centered on 12h00 at JFJ that are not seen at JER (figure 8), which we suggest result from local contamination related to the number of visitors and/or—less likely due to the missing correlation with CO—to the infrastructure. The detailed paths of these emissions are to be explained.

3.3. Investigation of potential triggers of the CO_2 spikes

Diurnal CO_2 spikes are only observed at JFJ, which means that periodic processes act on JFJ during the day as night values are similar to JER. This provides already an indication that the difference in elevation between the two measurement sites is not likely to play a major role. To further investigate the potential triggers for the CO_2 spikes, we used several meteorological parameters measured at the MeteoSwiss station Jungfraujoch (3580 m. a.s.l.). Among which air temperature, relative humidity, wind speed and sunshine duration show no covariations with the CO_2 spikes. Two other factors may suggest potential links: the global radiation and the wind direction.

Global radiation influences thermal uplift of the air and might influence the sites differently (e.g. Henne *et al* 2005). As seen on figure 4 and supplementary figure 1 for the summer season the CO_2 is not increasing synchronously and the amplitude appears to be independent from the absolute global radiation when global radiation is increasing early in the morning. Hence this parameter seems not to be the primary cause for the CO_2 spikes. Additionally, since the setting of the two stations is almost similar, global radiation should affect both sites to a similar degree, which is not the case. However, upwind regimes need some time to develop; thus, PBL injections will not appear immediately after sunrise.

Regarding the wind direction, a co-variability observed in January 2016 between wind direction and CO_2 excess is interesting as the direction varies only by $\pm10°$ and may be related to pollution originating from a local source. This co-variability is rarely seen in other periods. During Föhn days, we do not see any variations in the CO_2 excess values but we observe abrupt variations occurring simultaneously at the two locations (supplementary figure 1; section 4.2). Nevertheless, we think that due to its location in the saddle, the local wind regime may affect only JFJ through dilution. For instance, during the day and especially during the warm months, thermal air masses continuously pass over the Jungfrau saddle (i.e. JFJ) transporting polluted air from the surrounding valley without reaching JER (see also section 3.2).

The number of visitors is well in agreement with CO_2 excess spikes in summer. In winter, only disparate CO_2 excess values are observed or no excess at all as for example in January 2016 but also with only 100–200 visitors per hour (figure 4 and supplementary figure 1). In summer with up to 1000 passengers arriving per hour around noon, the anthropogenic influence is likely to be part of the emission source through direct as well as indirect influences. The visitors release CO_2 through breathing and smoke especially on the terrace below the laboratory's air inlet. People are mostly staying outside during sunny days, i.e. when the global radiation is high. Indirectly JFJ might also be influenced through the elevators that can act as chimneys uplifting local polluted air masses from the touristic complex (tunnels) or from maintenance or construction work at the infrastructure. In addition, activity related to the whole infrastructure is also enhanced when more visitors are onsite. It would be tempting to attribute most of the CO_2 excursions to local anthropogenic emission, nevertheless the lack of synchronicity for certain days tends to suggest that other parameters additionally influenced these diurnal excursions. The fact that all parameters (visitors, PBL, global radiation) have a diurnal behavior and also a pronounced seasonality makes it difficult to disentangle which one is acting as main contributor of the CO_2 spikes.

4. Summary and outlook

The following observations have been made:

- The comparison of CO_2 records over a 2 years period shows a good agreement between both sites. Especially in the night (00h00–06h00) values are indistinguishable within the measurement precision and establish that both sites are measuring robust atmospheric values.
- Daytime CO_2 spikes are not seen at JER, whereas cycles are often seen at JFJ, especially in summer.
- There is a distinct mean seasonal pattern with highest hourly CO_2 excess values of up to 1.3 ppm occurring around noon during the summer months.
- PBL injections seem to explain most of the daily to weekly variability. But there is also a possible influence of local anthropogenic contamination on CO_2 measurements at JFJ namely through the high number of visitors especially in summer or activities inherent to the infrastructure of the site.
- The low contaminated CO_2 and aerosol records establish JER as an additional site to perform high quality atmospheric measurements.

Yet, information panels about smoking effects on the touristic terrace are having a positive feedback on the observed excessive aerosol emissions documenting that the visitors read our information and react positively to lower emissions and help to improve our sensitive measurements (Bukowiecki *et al* 2021).

Here, we do not finish the discussion regarding the origin of these CO_2 spikes at JFJ as we cannot point to a single triggering cause. It probably results from a combination of factors, such as PBL variations—or more generally input of polluted air masses from the valley—local wind dynamics as well as the influence of visitors or infrastructure, especially in summer. Other competing factors (not revealed yet) might also likely to be involved. To minimize this influence, a new heated inlet system was placed ~80 m away from the tourist platform and is presently tested. Further studies may help to disentangle this issue, (a) a thorough investigation of local wind dynamics coupled to CO_2 profiles at both location, (b) ^{14}C measurements could highlight contamination by fossil fuel combustion emissions (Bozhinova *et al* 2014), (c) ^{13}C and O_2 measurements as indicator of biospheric sources may help to identify the origin of the contamination (Guillon *et al* 2015), (d) the comparison of high-quality water vapor concentration measurements at both location using humidity as a proxy for mountain venting processes (Henne *et al* 2005) and, thus, as a proxy for boundary layer influence (Cooper *et al* 2020) and (e) CO_2 monitoring in different locations of the station (touristic and meteo terraces, tunnel system) to see how coherent the variability is.

Finally, the CO_2 and the simultaneous aerosol studies (Bukowiecki *et al* 2021) highlight punctual anthropogenic pollution events and illustrate the sensitivity of instruments to anthropogenic activities at remote locations, with local contamination likely to be recorded by aerosols (Bukowiecki *et al* 2016), CO and to a certain extent in CO_2 records. In a rising tourism sector, spotting pollution events is a first step towards the quantification of anthropogenic gas emission related to the infrastructure, which would allow to provide solution for a good collaboration among all the involved stakeholders, i.e. scientists and tourism actors.

Data availability statement

The data that support the findings of this study are openly available at the following URL/DOI: https://gaw.kishou.go.jp. The CO_2 record from JER is available upon request. See the companion paper for the eBC availability.

Acknowledgments

ORCID iDs

Stéphane Affolter ● https://orcid.org/0000-0002-6646-9018
Nicolas Bukowiecki ● https://orcid.org/0000-0002-2925-8553

References

Balsiger H and Flückiger E 2016 The high altitude research station Jungfraujoch—the early years *From Weather Observations to Atmospheric and Climate Sciences in Switzerland* ed S W A M Furger (Zürich: vdf Hochschulverlag AG) pp 351–60

Baltensperger U, Gaggeler H W, Jost D T, Lugauer M, Schwikowski M, Weingartner E and Seibert P 1997 Aerosol climatology at the high-alpine site Jungfraujoch, Switzerland *J. Geophys. Res. Atmos.* **102** 19707–15

Bozhinova D, van der Molen M K, van der Velde I R, Krol M C, van der Laan S, Meijer H A J and Peters W 2014 Simulating the integrated summertime delta(CO_2)-C-14 signature from anthropogenic emissions over Western Europe *Atmos. Chem. Phys.* **14** 7273–90

Buchmann B, Baltensperger U, Calpini B, Leuenberger M, Flückiger E and Martin C E 2015 White paper. Research at Jungfraujoch—vision and mission statement 2015–2050 (*Bern: Swiss Academy of Sciences*)

Buchmann B, Hueglin C, Reimann S, Vollmer M K, Steinbacher M and Emmenegger L 2016 Reactive gases, ozone depleting substances and greenhouse gases *From Weather Observations and Atmospheric and Climate Sciences in Switzerland* ed S W A M Furger (Zürich: vdf Hochschulverlag AG) pp 361–74

Bukowiecki N, Brem B, Wehrle G, Močnik G, Affolter S, Leuenberger M, Collaud Coen M, Hervo M, Baltensperger U and Gysel-Beer M 2021 Elucidating local pollution and site representativeness at the Jungfraujoch, Switzerland through parallel aerosol measurements at an adjacent mountain ridge *Environ. Res. Commun.* **3** 021001

Bukowiecki N, Weingartner E, Gysel M, Collaud Coen M, Zieger P, Herrmann E, Steinbacher M, Gaggeler H W and Baltensperger U 2016 A review of more than 20 years of aerosol observation at the high altitude research station Jungfraujoch, Switzerland (3580 m asl) *Aerosol Air Qual. Res.* **16** 764–88

Cooper O R *et al* 2020 Multi-decadal surface ozone trends at globally distributed remote locations *Elem. Sci. Anthropocene* **8** 23

Dils B, Cui J, Henne S, Mahieu E, Steinbacher M and de Maziere M 2011 1997–2007 CO trend at the high Alpine site Jungfraujoch: a comparison between NDIR surface *in situ* and FTIR remote sensing observations *Atmos. Chem. Phys.* **11** 6735–48

Ferrarese S *et al* 2015 Inspection of high-concentration CO_2 events at the Plateau Rosa Alpine station *Atmos. Pollut. Res.* **6** 415–27

Friedlingstein P *et al* 2019 Global carbon budget 2019 *Earth Syst. Sci. Data* **11** 1783–838

Frohlich R *et al* 2015 Fourteen months of on-line measurements of the non-refractory submicron aerosol at the Jungfraujoch (3580 m a.s.l.)—chemical composition, origins and organic aerosol sources *Atmos. Chem. Phys.* **15** 11373–98

Fu X W, Marusczak N, Wang X, Gheusi F and Sonke J E 2016 Isotopic composition of gaseous elemental mercury in the free troposphere of the Pic du Midi observatory, France *Environ. Sci. Technol.* **50** 5641–50

Griffiths A D, Conen F, Weingartner E, Zimmermann L, Chambers S D, Williams A G and Steinbacher M 2014 Surface-to-mountaintop transport characterised by radon observations at the Jungfraujoch *Atmos. Chem. Phys.* **14** 12763–79

Guillon S, Agrinier P and Pili E 2015 Monitoring CO_2 concentration and delta C-13 in an underground cavity using a commercial isotope ratio infrared spectrometer *Appl. Phys.* B **119** 165–75

Henne S, Brunner D, Folini D, Solberg S, Klausen J and Buchmann B 2010 Assessment of parameters describing representativeness of air quality *in-situ* measurement sites *Atmos. Chem. Phys.* **10** 3561–81

Henne S, Furger M and Prevot A S H 2005 Climatology of mountain venting-induced elevated moisture layers in the lee of the Alps *J. Appl. Meteorol.* **44** 620–33

HFSJG 2019 Activity report 2018, international foundation high altitude research stations Jungfraujoch and Gornergrat (available at: www.hfsjg.ch)

IPCC 2013 Climate change 2013: the physical science basis *Contribution of Working Group I to the Fifth Assessment Report of the Intergovernmental Panel on Climate Change* (Cambridge: Cambridge University Press)

Kirkby J *et al* 2016 Ion-induced nucleation of pure biogenic particles *Nature* **533** 521

Loov J M B, Henne S, Legreid G, Staehelin J, Reimann S, Prevot A S H, Steinbacher M and Vollmer M K 2008 Estimation of background concentrations of trace gases at the Swiss Alpine site Jungfraujoch (3580 m asl) *J. Geophys. Res. Atmos.* **113** D22305

Mahieu E *et al* 2017 Retrieval of HCFC-142b (CH_3CClF_2) from ground-based high-resolution infrared solar spectra: atmospheric increase since 1989 and comparison with surface and satellite measurements *J. Quant. Spectrosc. Radiat. Transfer* **186** 96–105

Petzold A *et al* 2013 Recommendations for reporting 'black carbon' measurements *Atmos. Chem. Phys.* **13** 8365–79

Poltera Y, Martucci G, Collaud Coen M, Hervo M, Emmenegger L, Henne S, Brunner D and Haefele A 2017 PathfinderTURB: an automatic boundary layer algorithm. Development, validation and application to study the impact on *in situ* measurements at the Jungfraujoch *Atmos. Chem. Phys.* **17** 10051–70

Ruckstuhl A F, Henne S, Reimann S, Steinbacher M, Vollmer M K, O'Doherty S, Buchmann B and Hueglin C 2012 Robust extraction of baseline signal of atmospheric trace species using local regression *Atmos. Meas. Tech.* **5** 2613–24

Schibig M F, Mahieu E, Henne S, Lejeune B and Leuenberger M C 2016 Intercomparison of *in situ* NDIR and column FTIR measurements of CO_2 at Jungfraujoch *Atmos. Chem. Phys.* **16** 9935–49

Schibig M F, Steinbacher M, Buchmann B, van der Laan-luijkx I T, van der Laan S, Ranjan S and Leuenberger M C 2015 Comparison of continuous *in situ* CO_2 observations at Jungfraujoch using two different measurement techniques *Atmos. Meas. Tech.* **8** 57–68

Sturm P, Leuenberger M and Schmidt M 2005 Atmospheric O-2, CO_2 and delta C-13 observations from the remote sites Jungfraujoch, Switzerland, and Puy de Dome, France *Geophys. Res. Lett.* **32** L17811

Tröstl J *et al* 2016 The role of low-volatility organic compounds in initial particle growth in the atmosphere *Nature* **533** 527

Tsamalis C, Ravetta F, Gheusi F, Delbarre H and Augustin P 2014 Mixing of free-tropospheric air with the lowland boundary layer during anabatic transport to a high altitude station *Atmos. Res.* **143** 425–37

Uglietti C, Leuenberger M and Brunner D 2011 European source and sink areas of CO_2 retrieved from Lagrangian transport model interpretation of combined O-2 and CO_2 measurements at the high alpine research station Jungfraujoch *Atmos. Chem. Phys.* **11** 8017–36

van der Laan-luijkx I T *et al* 2013 Atmospheric CO_2, delta(O-2/N-2) and delta(CO_2)-C-13 measurements at Jungfraujoch, Switzerland: results from a flask sampling intercomparison program *Atmos. Meas. Tech.* **6** 1805–15

Vollmer M K, Reimann S, Hill M and Brunner D 2015 First observations of the fourth generation synthetic halocarbons HFC-1234yf, HFC-1234ze(E), and HCFC-1233zd(E) in the atmosphere *Environ. Sci. Technol.* **49** 2703–8

Vollmer M K, Reimann S, Hill M, Buchmann B and Emmenegger L 2016 Tracking new halogenated alkenes in the atmosphere *Chimia* **70** 365

WMO 2019 World meteorological organization: the state of greenhouse gases in the atmosphere based on global observations through 2018 *Greenhouse Gas Bulletin (GHG Bulletin)—No. 15*

WMO 2020 20th WMO/IAEA meeting on carbon dioxide, other greenhouse gases and related measurement techniques (GGMT-2019), Jeju Island, South Korea 2–5 September 2019 *GAW Report No. 255*

Yuan Y, Ries L, Petermeier H, Trickl T, Leuchner M, Couret C, Sohmer R, Meinhardt F and Menzel A 2019 On the diurnal, weekly, and seasonal cycles and annual trends in atmospheric CO_2 at Mount Zugspitze, Germany, during 1981–2016 *Atmos. Chem. Phys.* **19** 999–1012